Site-Directed Sulfhydryl Labeling of the Lactose Permease of *Escherichia coli*: Helix VII†

Pushpa Venkatesan,§ Isidore Kwaw,‡ Yonglin Hu, and H. Ronald Kaback*

Howard Hughes Medical Institute, Departments of Physiology and Microbiology & Molecular Genetics, Molecular Biology Institute, University of California—Los Angeles, Los Angeles, California 90095-1662

Received February 25, 2000; Revised Manuscript Received June 2, 2000

ABSTRACT: Site-directed sulfhydryl modification in situ is employed to investigate structural and dynamic features of transmembrane helix VII and the beginning of the periplasmic loop between helices VII and VIII (loop VII/VIII). Essentially all of the Cys-replacement mutants in the periplasmic half of the helix and the portion of loop VII/VIII tested are labeled by *N*-[^{14}C]ethylmaleimide (NEM). In contrast, with the exception of two mutants at the cytoplasmic end of helix VII, none of the mutants in the cytoplasmic half react with the alkylating agent. Labeling of most of the mutants is unaltered by ligand at 25 °C. However, at 4 °C, conformational changes induced by substrate binding become apparent. In the presence of ligand, permease mutants with a Cys residue at position 241, 242, 244, 245, 246, or 248 undergo a marked increase in labeling, while the reactivity of a Cys at position 238 is slightly decreased. Labeling of the remaining Cys-replacement mutants is unaffected by ligand. Studies with methanethiosulfonate ethylsulfonate (MTSES), a hydrophilic impermeant thiol reagent, show that most of the positions that react with NEM are accessible to MTSES; however, the two NEM-reactive mutants at the cytoplasmic end of helix VII and position 236 in the middle of the membrane-spanning domain are not. The findings demonstrate that positions in helix VII that reflect ligand-induced conformational changes are located in the periplasmic half and accessible to the aqueous phase from the periplasmic face of the membrane. In the following papers in this issue (Venkatesan, P., Lui, Z., Hu, Y., and Kaback H. R.; Venkatesan, P., Hu, Y., and Kaback H. R.), the approach is applied to helices II and X.

As one of the most extensively studied membrane transport proteins, the lactose permease (lac permease)[1] of *Escherichia coli* has emerged as a paradigm for secondary transport proteins that convert free energy stored in electrochemical ion gradients into work in the form of solute concentration gradients (*1*−*5*). Encoded by the *lacY* gene, the permease has been solubilized from the membrane, purified to homogeneity, reconstituted into proteoliposomes, and shown to be solely responsible for the coupled stoichiometric symport of galactosides and H^+ (reviewed in ref *6*) as a monomer (*7*). All available evidence indicates that the permease is composed of 12 hydrophobic, membrane-spanning, α-helical domains connected by relatively hydrophilic loops with both the N- and the C-termini on the cytoplasmic face of the membrane (Figure 1) (reviewed in refs *8* and *9*).

In a functional mutant devoid of native Cys residues, each residue has been replaced with Cys (reviewed in ref *10*). Analysis of the mutant library has led to the following developments (*9*−*12*): (i) The great majority of the mutants are expressed normally in the membrane and exhibit significant activity, and only six side chains are clearly irreplaceable with respect to active transport: Glu126 (helix IV) and Arg144 (helix V), which are indispensable for substrate binding, and Glu269 (helix VIII), Arg302 (helix IX), His322, and Glu325 (helix X), which are critical for H^+ translocation and coupling with substrate translocation. (ii) Helix packing, tilts, and ligand-induced conformational changes have been determined by using site-directed biochemical and biophysical techniques. (iii) Positions where the reactivity of the Cys replacement is increased or decreased by ligand binding have been identified. (iv) The permease has been shown to be a highly flexible molecule. (v) A working model describing a mechanism for lactose/H^+ symport has been formulated.

Site-directed sulfhydryl modification of single-Cys permease mutants in situ with *N*-ethylmaleimide (NEM) has been particularly useful for studying both static and dynamic features of lac permease (*13*−*15*), as well as a number of other membrane proteins (e.g., refs *16*, *17*−*25*). Alkylation with NEM is a measure of the reactivity and/or accessibility of a given Cys residue to this small, relatively hydrophobic, membrane-permeant thiol-specific reagent. Reactivity and/or accessibility is dependent primarily on the environment

† This work was supported in part by NIH Grant DK51131 to H.R.K.

* To whom correspondence should be addressed. HHMI/UCLA, 5-748 MacDonald Research Laboratories, Box 951662, Los Angeles, CA 90095-1662. Telephone: (310) 206-5053. Telefax: (310) 206-8623. E-mail: RonaldK@HHMI.UCLA.edu

§ P.V. is the recipient of NIH NRSA Postdoctoral Fellowship 5 F32 DK09287.

‡ I.K. is the recipient of a fellowship from the Robert Wood Johnson Foundation-Minority Medical Faculty Development Program.

[1] Abbreviations: lac permease, lactose permease; C-less permease, functional lac permease devoid of Cys residues; TDG, β,D-galactopyranosyl 1-thio-β,D-galactopyranoside; NEM, *N*-ethylmaleimide; MTSES, methanethiosulfonate ethylsulfonate; IPTG, isopropyl 1-thio-β,D-galactopyranoside; RSO, right-side-out; DTT, dithiothreitol; KP_i, potassium phosphate; DDM, *n*-dodecyl β,D-maltopyranoside; $NaDodSO_4$, sodium dodecyl sulfate.

10.1021/bi000438b CCC: $19.00
Published on Web 08/09/2000

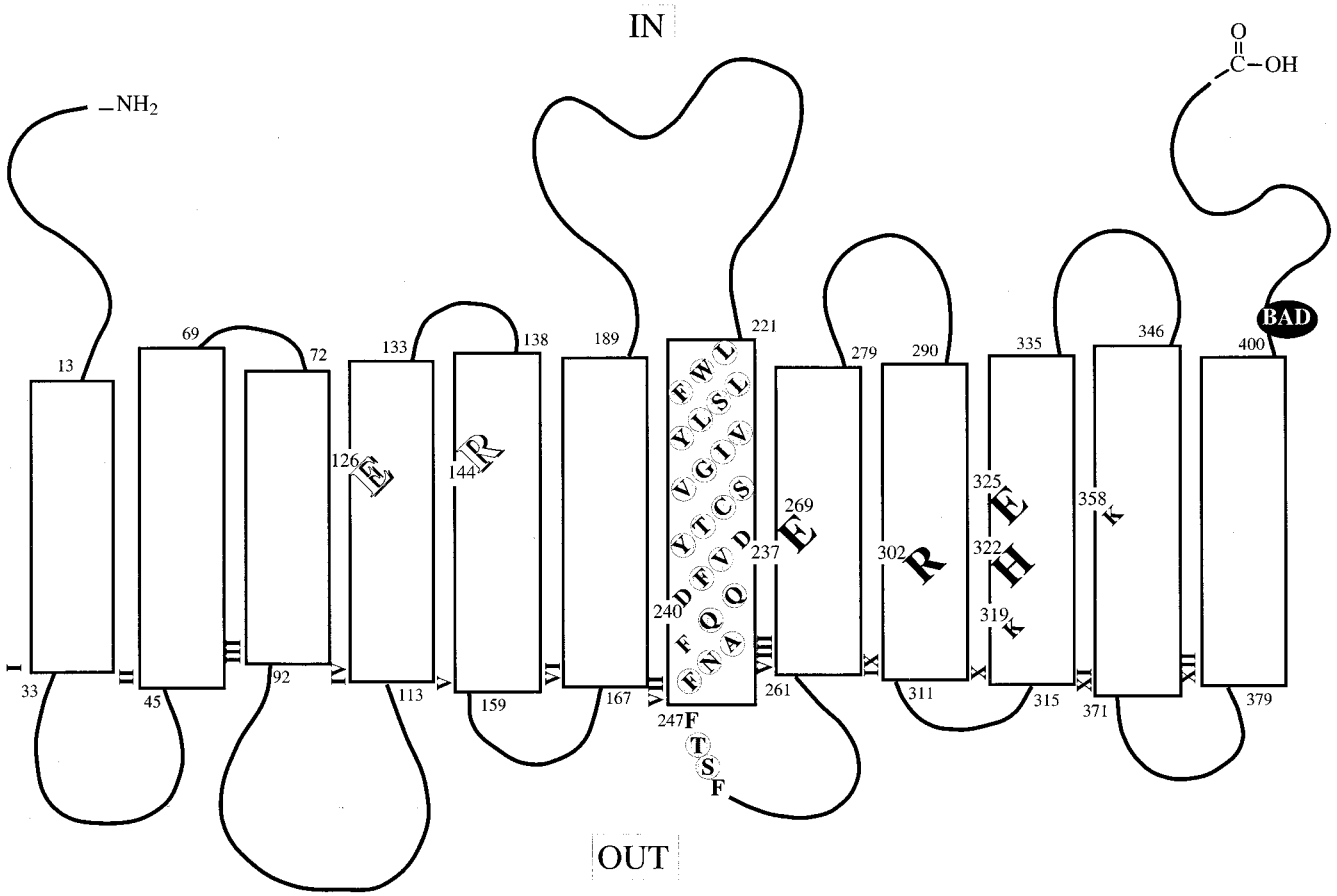

FIGURE 1: Secondary structure model of lac permease. Single-letter amino acid code is used, and putative transmembrane helices are shown in boxes. The six irreplaceable residues Glu126 (helix IV), Arg144 (helix V), Glu269 (helix VIII), Arg302 (helix IX), His322 (helix X), and Glu325 (helix X) are shown as enlarged Roman letters. In addition, the charge-pairs Asp237 (helix VII)/Lys358 (helix XI) and Asp240 (helix VII)/Lys319 (helix X) are shown. Residues in helix VII studied by site-directed NEM labeling are shown in shaded circles, and the site of the biotin acceptor domain (BAD) is indicated.

in the vicinity of a given Cys side chain and is limited by close tertiary contacts between transmembrane helices and steric constraints of the lipid bilayer. Hence, determination of the reactivity of Cys replacement mutants with NEM is convenient to assess the local environment of specific positions within the tertiary structure. On the other hand, in situ site-specific labeling with methanethiosulfonate ethylsulfonate (MTSES), a small hydrophilic, membrane-impermeant thiol reagent (*26*−*28*), has been utilized to study the accessibility of Cys residues in lac permease to the aqueous milieu (*29*). When extended to each transmembrane residue, the method should allow delineation of the solvent-filled cleft in the permease (*12*, *30*−*34*) that may represent all or part of the translocation pathway. Any change in labeling of a given Cys side chain upon substrate binding is indicative of an alteration in the local environment around the Cys residue. Hence, in situ labeling is valuable for identifying conformational alterations induced by ligand binding or other perturbants (*14*).

Transmembrane helix VII is centrally located amidst helices containing residues irreplaceable for active transport (*12*). Although the domain does not contain any of the six irreplaceable residues, many observations indicate that helix VII plays an important role with respect to structure and activity: (i) Cys-scanning mutagenesis of helix VII and the flanking hydrophilic loops reveals that positions where Cys replacements render the permease highly sensitive to inactivation by NEM are located in the periplasmic half, a region that is strongly conserved among transport proteins homologous to lac permease (*35*). (ii) The periplasmic half of helix VII also contains Asp237 and Asp240, which are charge-paired with Lys358 (helix XI) and Lys319 (helix X), respectively (*36*−*42*). (iii) The NEM reactivity of two Cys-replacement mutants in this domain (V238C and A244C)[2] is altered in the presence of substrate (*14*). (iv) The epitope for monoclonal antibody 4B1 that uncouples lactose from H^+ translocation (*43*, *44*) is composed of residues Phe247, Phe250, and Gly254 in the periplasmic loop between helices VII and VIII (loop VII/VIII) (*45*−*47*). (v) Site-directed spin-labeling studies demonstrate that transmembrane domain VII is an α-helix that makes contact with the neighboring domains in the tertiary structure (*47*). (vi) Certain replacements for Asp68 at the cytoplasmic end of helix II abolish activity, and in a number of revertants, the phenotype is suppressed by mutations in helix VII (*48*). (vii) Site-directed thiol cross-linking and other experiments (reviewed in ref *12*) indicate that the periplasmic half of helix VII is proximal to helices I, II, III, IV, V, X, and XI; ligand binding increases the distance between helices VII and I or II at the periplasmic

[2] Site-directed mutants are designated by the single-letter amino acid abbreviation for the targeted residue, followed by the sequence position of the residue in the wild-type lac permease and followed by a second letter indicating the amino acid replacement.

ends (*49*−*51*); and conformational flexibility between helices VII and I or II is important for turnover (*49*).

In this paper, site-directed NEM labeling in situ is used to study transmembrane helix VII. The results support the conclusion that the periplasmic half of helix VII is conformationally active and demonstrate further that this half of helix VII is accessible to the aqueous phase from the periplamic face of the membrane.

EXPERIMENTAL PROCEDURES

Materials. N-[*ethyl*-1-^{14}C]Ethylmaleimide (40 mCi/mmol) was purchased from DuPont NEN (Boston, MA). [^{125}I]Protein A was from Amersham (Arlington Heights, IL). Immobilized monomeric avidin was from Pierce (Rockford, IL). MTSES was purchased from Toronto Research Chemicals (Toronto, Ontario, Canada). Site-directed rabbit polyclonal antiserum against a dodecapeptide corresponding to the C-terminus of lac permease was prepared as described (*52*). All other materials were reagent-grade and obtained from commercial sources.

Plasmid Construction. Construction of the single-Cys mutants used and insertion of the DNA fragment encoding the biotin acceptor domain from a *Klebsiella pneumoniae* oxaloacetate decarboxylase at the C-terminus of the mutants by restriction fragment replacement has been described (*35*, *47*). Each mutant was verified by using the dideoxynucleotide termination method (*53*). Permease mutants F243C and F247C are not alkylated by NEM (*14*) and were omitted from this study. The Asp residues at positions 237 and 240, which are charge-paired with Lys358 and Lys319, respectively, were also not investigated, as previous studies (*40*) demonstrate that Cys residues at these positions can be modified by either iodoacetic acid or MTSES.

Growth of Bacteria. E. coli T184 (*lacY*$^{-}$*Z* $^{-}$*)* transformed with a plasmid encoding a given mutant was grown aerobically at 37 °C in Luria−Bertani broth containing streptomycin (10 μg/mL) and ampicillin (100 μg/mL). Fully grown cultures were diluted 10-fold and grown for 2 h before induction with 0.5 mM isopropyl 1-thio-β,D-galactopyranoside. After additional growth for 2 h, cells were harvested and used for the preparation of right-side-out (RSO) membrane vesicles.

Preparation of RSO Membrane Vesicles. RSO membrane vesicles were prepared from 4-L cultures of *E. coli* T184 expressing a given mutant by lysozyme-ethylenediaminetetraacetic acid treatment and osmotic lysis (*54*, *55*). The vesicles were resuspended at a protein concentration of 16−22 mg/mL in 100 mM potassium phosphate (KP_i; pH 7.5)/10 mM $MgSO_4$, frozen in liquid N_2, and stored at −80 °C until use.

NEM Labeling. Alkylation with [^{14}C]NEM was performed essentially as described (*13*). RSO membrane vesicles [0.4 mg of protein in 50 μL of 100 mM KP_i (pH 7.5)/10 mM $MgSO_4$] harboring a given single-Cys permease mutant were incubated with [^{14}C]NEM (40 mCi/mmol; 0.4 mM final concentration) in the absence or presence of 10 mM TDG at 4 or 25 °C as indicated. Labeling was terminated after 10 min by the addition of 15 mM dithiothreitol (DTT), and the membranes were solubilized with 2.0% (w/v) *n*-dodecyl-β,D-maltopyranoside (DDM) for 5 min at 25 °C. The DDM extract containing solubilized membranes was incubated with immobilized monomeric avidin-Sepharose previously equilibrated in 50 mM KP_i (pH 7.5)/150 mM NaCl/0.02% DDM (w/v; equilibration buffer) for 30 min at 4 °C. The resin was then extensively washed with equilibration buffer, and biotinylated permease was eluted with 5 mM D-biotin in equilibration buffer. Sodium dodecyl sulfate/12% polyacrylamide gel electrophoresis ($NaDodSO_4$/PAGE) followed by autoradiography was used to analyze NEM labeling. The relative amounts of autoradiographic bands were quantitated with a STORM 860 Phosphoimager (Molecular Dynamics).

MTSES Labeling. RSO membrane vesicles [0.5−0.6 mg of protein in 50 μL of 100 mM KP_i (pH 7.5)/10 mM $MgSO_4$] harboring a given single-Cys permease mutant were incubated without or with methanethiosulfonate ethylsulfonate (MTSES; 200 μM final concentration) for 5 min at 25 °C in the absence or presence of 10 mM TDG, as indicated. After washing twice with 1 mL of ice-cold 100 mM KP_i (pH 7.5)/10 mM $MgSO_4$ to remove excess MTSES and TDG, the vesicles were resuspended in 50 μL of the same buffer. TDG (10 mM final concentration) was added back to the samples treated originally with TDG, and the samples were incubated with [^{14}C]NEM (40 mCi/mmol; 0.4 mM final concentration) for 30 min at 25 °C. The reaction was quenched with DTT, and the permease was solubilized, purified, and subjected to $NaDodSO_4$/PAGE. Analysis of the autoradiographic bands was used to evaluate the extent of MTSES labeling that corresponds to a decrease in the intensity of [^{14}C]NEM-labeled permease in samples treated with MTSES relative to the untreated samples.

Western Blot Analysis. Fractions containing affinity-purified biotinylated permease were analyzed by $NaDodSO_4$/PAGE (*56*). Protein was electroblotted on to poly(vinylidene difluoride) membranes (Immobilon-PVDF; Millipore) and probed with a site-directed polyclonal antibody against the C-terminus of lac permease (*52*). The PVDF membrane was subsequently incubated with [^{125}I]protein A (30 mCi/mg, 100 μCi/mL) and autoradiographed. Quantification of the relative amounts of permease was carried out with a STORM 860 Phosphoimager (Molecular Dynamics).

Protein Determinations. Protein was assayed using a Micro BCA protein determination kit (Pierce Inc., Rockford, IL).

RESULTS

NEM Labeling at 25 °C. Permease mutants with a single-Cys residue at positions throughout helix VII and the beginning of loop VII/VIII (Figure 1) were subjected to site-directed alkylation with [^{14}C]NEM in RSO vesicles in the absence or presence of the high-affinity substrate analogue β,D-galactopyranosyl 1-thio-β,D-galactopyranoside (TDG) (*13*, *14*, *29*). Mutants L222C, F224C, Y236C, V238C, Q241C, Q242C, A244C, N245C, F246C, and S249C label readily with NEM in 10 min at 25 °C (Figure 2, lane 3 in the appropriate panels). Labeling of position 222, 224, 236, 242, 244, 245, 246, or 249 is essentially unchanged in the presence of TDG (compare lanes 3 and 4 in the appropriate panels), implying either that TDG does not induce a conformational change reflected at these positions or that the induced change is not apparent at 25 °C. TDG slightly attenuates alkylation of V238C permease, causes a mild increase in labeling of mutant Q241C, and stimulates labeling of T248C permease approximately 7-fold (lanes 3 and 4 in

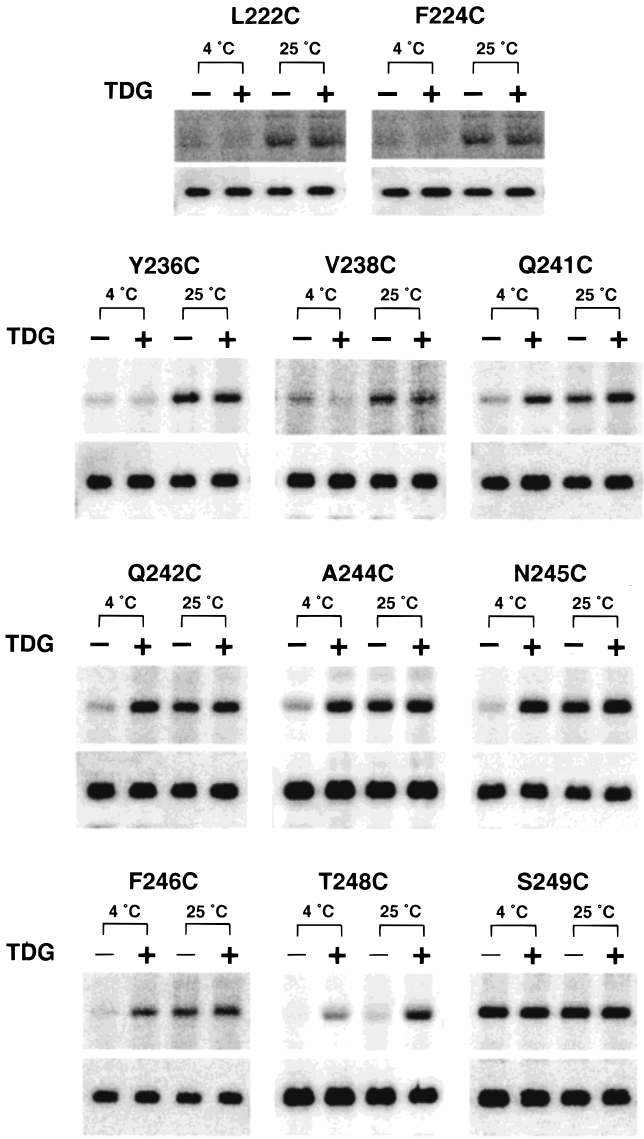

FIGURE 2: Effect of TDG and temperature on NEM labeling of given single-Cys mutants in RSO membrane vesicles. RSO membrane vesicles [0.4 mg of protein in 50 μL of 100 mM KP_i (pH 7.5)/10 mM $MgSO_4$] prepared from *E. coli* T184 transformed with a plasmid encoding an indicated single-Cys mutant were incubated with [^{14}C]NEM (40 mCi/mmol; 0.4 mM final concentration) for 10 min in the absence or presence of 10 mM TDG at 4 or 25 °C as shown. Reactions were terminated with DTT (15 mM final concentration), and biotinylated permease was solubilized and purified by avidin-affinity chromatography as described in Experimental Procedures. Aliquots containing approximately 5 μg of protein were separated, $NaDodSO_4$/12% PAGE, and the labeled protein was visualized by autoradiography (upper panels). A fraction of the protein (0.5 μg) eluted from the avidin-Sepharose beads was analyzed by Western blotting with anti-C-terminal antibody to quantify the amount of permease in each sample (lower panels).

the appropriate panels). Mutants W223C, L225C, S226C, L227C, Y228C, V229C, I230C, G231C, V232C, CS233C, C234, T235C, and F239C are not alkylated by NEM during a 10-min reaction period in the absence or presence of TDG, suggesting that the Cys side chain at these positions is in an environment that is sterically and/or electronically unfavorable for reactivity (data not shown).

NEM Labeling at 4 °C. To determine if ligand-induced conformational changes can be detected by decreasing the thermal motion of the protein, in situ labeling was also carried out at 4 °C (*49*, *57*). With S249C permease, NEM labeling at 4 °C is efficient, comparable to that observed at 25 °C (Figure 2, panel S249C, compare lanes 1 and 3), and no significant change is observed in the presence of TDG (compare lanes 1 and 2). Therefore, when NEM reacts relatively rapidly with an accessible sulfhydryl group, lowering the temperature to 4 °C does not significantly decrease labeling over a 10-min reaction period. It follows that any difference in NEM labeling at 4 °C relative to 25 °C is likely due to a change in the environment of the cysteinyl side chain arising from decreased thermal motion of the protein. Labeling of L222C, F224C, Y236C, V238C, Q241C, Q242C, A244C, N245C, or F246C is markedly lower at 4 °C as compared to that observed at 25 °C, presumably reflecting decreased thermal motion of the protein (compare lanes 1 and 3 in the appropriate panel).

Strikingly, ligand-induced conformational changes that were imperceptible at 25 °C are clearly perceived at 4 °C with many of the mutants (Figure 2, lanes 1 and 2). In the presence of TDG, a pronounced increase in labeling is observed at 4 °C with permease mutants Q241C, Q242C, A244C, N245C, and F246C (Figure 2, compare lanes 1 and 2 in the appropriate panels). Interestingly, in the presence of TDG, labeling at 4 or 25 °C is comparable (compare lanes 2 and 4), indicating that labeling in the presence of ligand is independent of local thermal motion. This finding is in contrast to the marked differential labeling observed at the two temperatures in the absence of ligand with these mutants (compare lanes 2 and 4 and contrast with lanes 1 and 3). Low temperature also decreases NEM labeling in mutants Y236C, V238C, or T248C, and ligand does not alter labeling of Y236C permease. Although labeling of V238C permease is relatively weak at 4 °C, significant attenuation of labeling is observed in the presence of ligand that is not as obvious at 25 °C. With mutant T248C, labeling in the presence of substrate is clearly more pronounced at 25 °C than at 4 °C, suggesting that increased labeling at higher temperature may be due primarily to increased conformational flexibility (panel T248C, compare lanes 2 and 4).

MTSES Accessibility. Permease mutants that react with NEM in RSO vesicles were tested for accessibility to MTSES, a hydrophilic sulfhydryl reagent used to study accessibility of Cys residues to water (*13*, *26*−*29*). Pretreatment of L222C, F224C, or Y236C permease with MTSES either in the absence or presence of TDG has no effect on NEM labeling, indicating that these positions are inaccessible to solvent (Figure 3, appropriate panels). NEM labeling of V238C permease is partially decreased after preincubation with MTSES, indicating that position 238 is partially solvent-exposed (V238C, lanes 1 and 3). In addition, there appears to be a further decrease in labeling of this mutant when MTSES treatment is carried out in the presence of TDG, implying that TDG may increase solvent accessibility to a small extent. Mutants Q241C, Q242C, A244C, N245C, F246C, and S249C are accessible to MTSES either in the presence or absence of ligand as shown by the decrease in NEM labeling after pretreatment with MTSES (Figure 4, appropriate panels). Interestingly, taking into account dif-

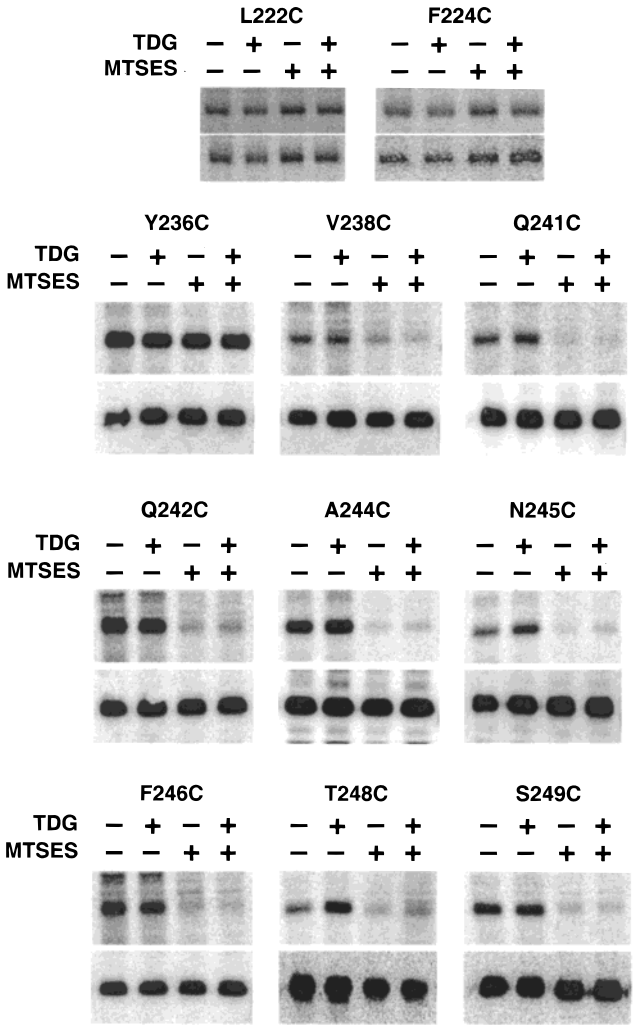

FIGURE 3: Accessibility of given single-Cys permease mutants to MTSES and the effect of TDG. RSO membrane vesicles (0.5−0.6 mg of protein in 0.5 mL of 100 mM KP_i (pH 7.5)/10 mM $MgSO_4$) prepared from *E. coli* T184 transformed with plasmid encoding the indicated single-Cys mutant were incubated without or with MTSES (200 μM final concentration) for 5 min at 25 °C in the absence or presence of TDG, as indicated. Vesicles were washed twice with ice-cold buffer and resuspended in 50 μL of the same buffer, and TDG (10 mM final concentration) was added back to the samples initially treated with TDG. Samples were then treated with [^{14}C]NEM (40 mCi/mmol; 0.4 mM final concentration) for 30 min at 25 °C. Reactions were quenched with DTT, and biotinylated permease was solubilized and purified as described in Experimental Procedures. Aliquots containing approximately 5 μg of protein were separated by $NaDodSO_4$/12% PAGE, and the NEM-labeled protein was visualized by autoradiography (upper panels). A fraction of the protein (0.5 μg) eluted from the avidin-Sepharose beads was analyzed by Western blotting with anti-C-terminal antibody to quantify the amount of permease in the samples (lower panels).

ferences in permease concentration (T248C; bottom),[3] NEM labeling of T248C permease is essentially unchanged by pretreatment with MTSES, but in the presence of TDG, Cys248 becomes more accessible to solvent, as evidenced by a 2−3-fold decrease in the enhanced labeling observed in the presence of ligand and MTSES (compare lanes 1 and 2 to lanes 3 and 4). Thus, positions 222, 224, and 236 are inaccessible to solvent; position 238 is partially accessible from the periplasmic face of the membrane; positions 241, 242, 244, 245, 246, and 249 are significantly more accessible; and position 248 becomes more exposed in the presence of ligand.

[3] Relative protein concentrations in this panel, as quantitated by phosphorimaging, are 1.0, 1.0, 0.5, and 0.5 for lanes 1, 2, 3, and 4, respectively.

DISCUSSION

Cys-scanning mutagenesis of transmembrane helix VII demonstrates that the eight positions where Cys replacements cause the permease to be inactivated by NEM are located in the periplasmic half of helix VII (*35*). Further site-specific sulhydryl modification studies in situ indicate that three single-Cys mutants—V238C, A244C and T248C—exhibit altered reactivity to NEM in the presence of substrate, while mutants F243C and F247C are not alkylated (*14*). The work presented here extends in situ site-directed labeling to the remainder of helix VII, as well as to the beginning of loop VII/VIII, and documents the solvent accessibility of this region. As shown, 10 of the 24 single-Cys replacement mutants studied label with NEM at 25 °C (Figure 4). A majority of the mutants do not exhibit significant ligand-induced conformational changes at 25 °C. However, when alkylation is carried out at 4 °C where thermal motion of the protein is minimized, conformational alterations resulting from substrate binding become apparent. Thus, in the presence of TDG, positions 241, 242, 244, 245, and 246 at the periplasmic end of the helix, as well as 248 in loop VII/VIII, undergo dramatic increases in NEM labeling, indicating a marked change in the environment in the vicinity of the Cys side chains at these positions. Position 238, on the other hand, appears to undergo a decrease in accessibility in the presence of TDG. Permease mutants L222C and F224C at the cytoplasmic end of helix VII, Y236C in the approximate middle and S249C in loop VII/VIII do not display any TDG-induced alteration in NEM labeling. The remaining mutants (W223C, L225C, S226C, L227C, Y228C, V229C, I230C, G231C, V232C, S233C, C234, and T235C), all of which are in the cytoplasmic half of the transmembrane domain, do not label either in the absence or presence of ligand. The results demonstrate that those positions that reflect structural changes induced by substrate binding are situated in the periplasmic half of helix VII and are consistent with Cys-scanning mutagenesis studies (*35*), indicating that this portion of the transmembrane domain is important for function.

A variety of biochemical and biophysical studies demonstrate that the approximate periplasmic half of helix VII is surrounded by transmembrane domains I, II, III, IV, V, X, and XI (*49*−*51*, *58*−*64*) (*12*). Furthermore, binding of TDG causes a scissors-like or translational movement between helix VII and helices I or II that increases interhelical distances at the periplasmic ends (*49*−*51*). Accordingly, the present study shows that ligand binding causes residues at the periplasmic end of helix VII to label more readily with NEM (Figure 4). TDG also enhances labeling of residues located in the periplasmic end of helices I (*65*) and II (Venkatesan, P., Lui, Z., Hu, Y., and Kaback H. R., in the following paper in this issue). Evidence that helix VII is relatively sequestered within the tertiary structure is derived from site-directed spin-labeling studies (*47*) showing that spin-labeled side chains within helix VII have low average mobility and accessibility to oxygen. In addition, thiol cross-

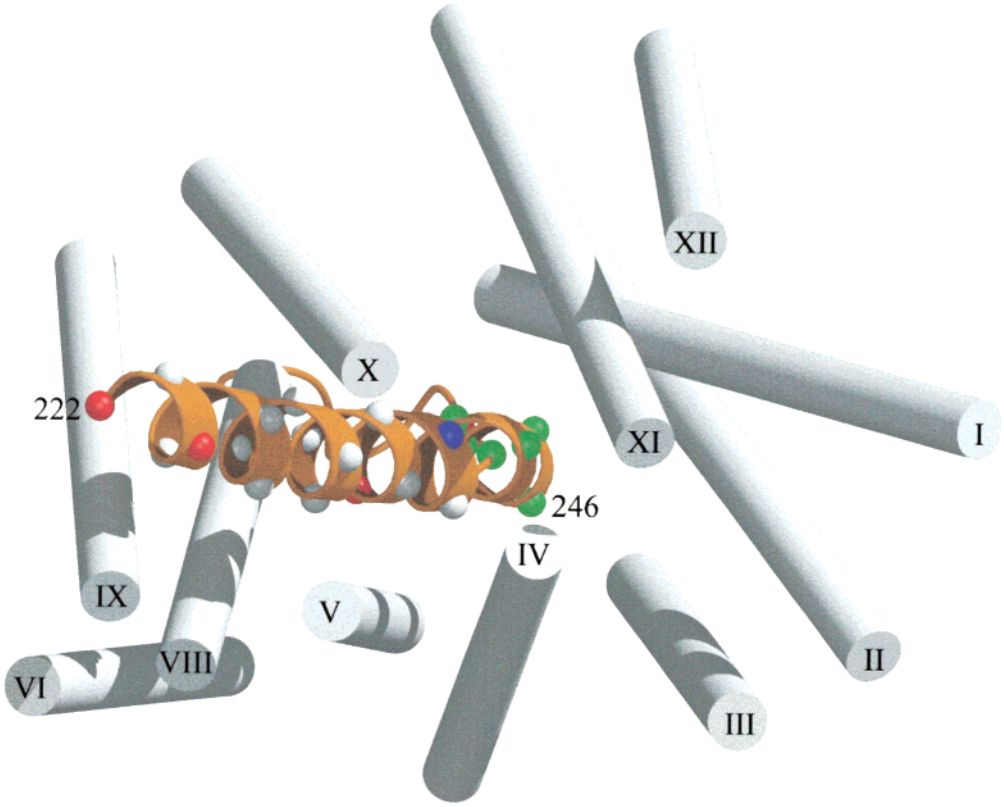

FIGURE 4: NEM labeling and the effect of ligand on single-Cys replacements in helix VII. Results from Figure 2 are shown in a 3D representation of helix VII as follows. Positions that label with NEM are presented as colored spheres: red, labels with NEM with no change in the presence of TDG; green, increased labeling in the presence of TDG; blue, decreased labeling in the presence of TDG. Positions that do not label are shown as white spheres. Helices other than helix VII are shown as rods, and their positions are derived from modeling studies (*69*) using approximately 100 constraints (*12*).

linking experiments indicate that helices I, II, and V tilt away from helix VII toward the cytoplasmic side of the membrane (*50*, *51*, *62*) and that helix IV crosses helix VII in scissors-like fashion at the approximate middle of the membrane (*61*). It is highly likely that this tertiary packing arrangement is responsible for the decreased NEM reactivity of Cys residues in the cytoplasmic half of VII.

Three distinct patterns of alkylation of single-Cys replacement mutants by NEM are observed in this study: (i) Absence of labeling indicating inaccessibility or low reactivity of the Cys side chain. (ii) High reactivity at 25 °C and a low reactivity at 4 °C, implying that accessibility to NEM is due largely to thermal motion of the protein. (iii) Comparable labeling at 25 °C and 4 °C, suggesting that labeling is independent of protein thermal motion. These patterns indicate qualitatively the contribution of the thermal motion to accessibility at each site. A relatively high degree of thermal motion appears to be responsible for the high reactivity of Cys residues at positions 222, 224, 236, 241, 242, 244, 245, and 246 at 25 °C and markedly low reactivity at 4 °C (Figure 2). However, in the presence of TDG, the intensity of labeling observed at the two temperatures is comparable and high for Cys residues at positions 241, 242, 244, 245, and 246, indicating that NEM labeling is independent of protein thermal motion when ligand is bound. As shown previously, permease mutant T248C, with negligible reactivity with NEM at room temperature, exhibits a dramatic increase in NEM labeling in the presence of TDG. Interestingly, enhanced labeling is more pronounced at 25 °C than at 4 °C, suggesting that the effect is due primarily to protein thermal motion. On the other hand, the strong and equal extent of labeling of the Cys residue in S249C permease at both temperatures indicates that position 249 in periplasmic loop VII/VIII is very accessible to the reagent and that accessibility is independent of protein dynamics. Taken together, the observations demonstrate that despite being flanked by several helices in the tertiary structure, the periplasmic half of helix VII has a significant degree of flexibility that confers accessibility to NEM. Thermal motion of the protein that contributes to this structural flexibility may not allow detection of ligand-induced alterations in NEM labeling, particularly if the degree of the conformational change falls within the range of protein thermal motion. Lowering the temperature of the labeling reaction decreases thermal motion and conformational flexibility, thereby facilitating detection of substrate-induced conformational changes at positions highly accessible to thiol reagents.

Accessibility studies with the hydrophilic probe MTSES (*26*, *28*) accentuate the structural importance of the periplasmic half of helix VII. With the exception of Y236C and T248C, all the Cys-replacement mutants alkylated by NEM are accessible to MTSES and therefore to bulk solvent from the periplasmic side of the membrane (Figure 5). Positions 238, 241, 242, 244, 245, 246, and 249 are solvent-accessible in the absence or presence of TDG, while position 248 becomes accessible to the aqueous medium upon substrate binding. Position 236, which is not labeled by MTSES, and positions 233, 239, 243, and 247, which are not labeled by NEM, are situated on one face of helix VII, whereas positions accessible to solvent (i.e., blocked by MTSES) are located

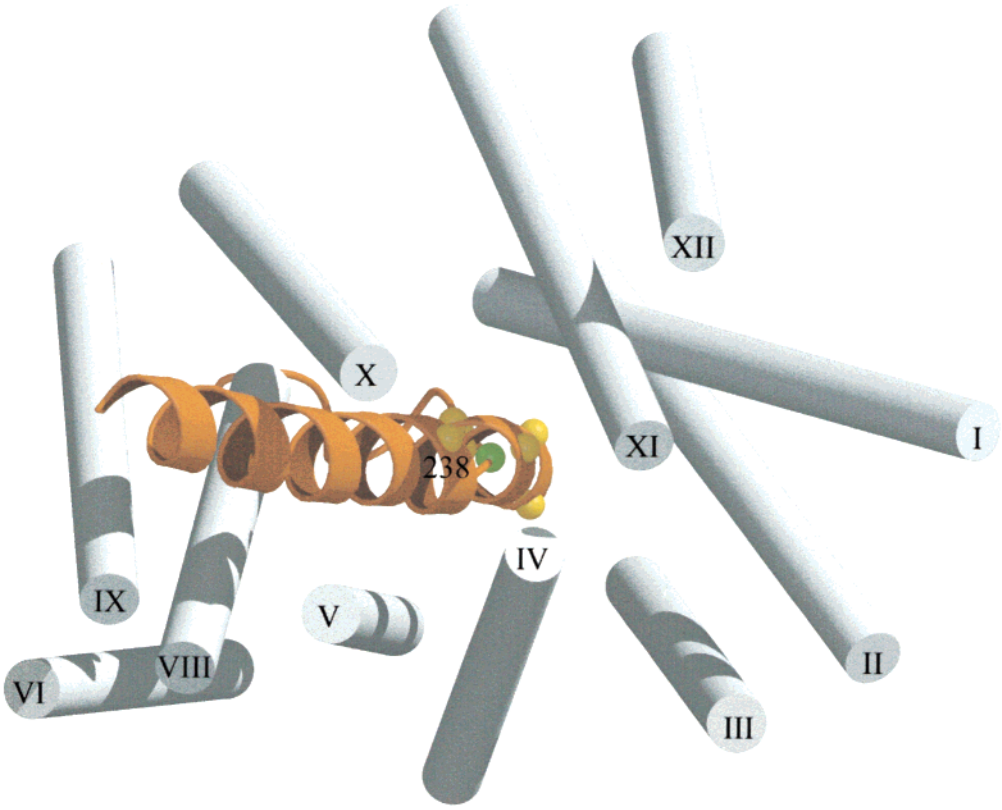

FIGURE 5: Solvent accessibility of single-Cys replacements in helix VII as judged by MTSES blockade of NEM labeling. Results from Figure 3 are shown in a 3D representation of helix VII. Positions where NEM labeling is significantly blocked by MTSES are shown as yellow spheres. Position 248 is represented as a green sphere to indicate increased accessibility to solvent in the presence of TDG. Helices other than helix VII are shown as rods, and their positions are derived from modeling studies (*69*) using approximately 100 constraints (*12*).

on the opposite face of the periplasmic half of helix VII. Charge-scanning studies with wild-type lac permease show that Asn245, Phe246, Thr248, and Ser249 can be individually replaced with Glu or Arg without significant loss of active transport, suggesting that exposure to solvent allows these positions to accommodate a charged residue (C. D. Wolin and H.R.K., unpublished observations). However, site-directed spin-labeling (*47*) indicates that nitroxide-labeled side chains at intramembrane positions 233−246 that exhibit a low collision frequency with the polar relaxation agent potassium chromium oxalate (CrOx) are inaccessible to solvent. On the other hand, nitroxide-labeled residues at surface-exposed positions 247−255 that display a high collision frequency with CrOx are accessible to bulk water. The results reported here for MTSES support the charge-scanning data by confirming that positions 245 and 246 are solvent-exposed and further demonstrate that four additional positions within the transmembrane region are also accessible to the periplasmic aqueous phase. It is noteworthy that the relative accessibility of spin-labeled side chains to CrOx or O_2 may be more appropriate for studying membrane protein topology (*66*, *67*) than for delineating solvent-accessible positions within transmembrane domains. Site-directed MTSES labeling in situ may reflect solvent-exposed positions more accurately because MTSES is more likely to diffuse into water-filled crevices within the transmembrane regions of the protein than CrOx, which is a bulkier molecule, and labeling of a Cys residue in situ with a hydrophilic thiol reagent such as MTSES is a more direct way to estimate accessibility of a given position to water than studying the collision frequency of nitroxide-labeled Cys side chain with CrOx in DDM micelles. In any case, the high degree of solvent accessibility of the periplasmic half of helix VII reported here correlates well with the finding that most of the protein backbone is accessible to water as indicated by the observation that over 80% of the backbone amide protons in the permease exchange with deuterium within 10 min (*68*).

A water-filled notch or cleft in the permease, presumably caused by tilting of transmembrane helices (*62*), has been observed by electron microscopy (*30*−*34*). The results presented here indicate that Val238, Gln241, Gln242, Ala244, Asn245, and Phe246 in helix VII, which are accessible from the aqueous phase at the periplasmic side of the membrane, line part of the cleft. Furthermore, the finding that these same positions also reflect conformational alterations produced by ligand binding lends credence to the notion that the hydrophilic cleft may be related to the substrate and/or H^+ translocation pathway. Recently, a helix packing model of lac permease depicting the packing and tilts of individual helices with respect to one another, as well as the putative solvent-filled cleft, has been formulated based upon thiol-cross-linking and other site-directed approaches (reviewed in ref *12*). Additional details regarding each position within the permease and its dynamics are currently being acquired by systematic site-directed sulfhydryl labeling in situ as illustrated in this and in the following papers in this issue (Venkatesan, P., Lui, Z., Hu, Y., and Kaback H. R.; Venkatesan, P., Hu, Y., and Kaback H. R.).

ACKNOWLEDGMENT

We are deeply indebted to Mark Girvin for molecular modeling. In addition, we thank Kerstin Stempel for help with the preparation of the figures.

REFERENCES

1. Kaback, H. R. (1976) *J. Cell. Physiol. 89*, 575−593.
2. Kaback, H. R. (1983) *J. Membr. Biol. 76*, 95−112.
3. Kaback, H. R. (1989) *Harvey Lect. 83*, 77−103.
4. Poolman, B., and Konings, W. N. (1993) *Biochim. Biophys. Acta 1183*, 5−39.
5. Varela, M. F., and Wilson, T. H. (1996) *Biochim. Biophys. Acta 1276*, 21−34.
6. Viitanen, P., Newman, M. J., Foster, D. L., Wilson, T. H., and Kaback, H. R. (1986) *Methods Enzymol. 125*, 429−452.
7. Sahin-Tóth, M., Lawrence, M. C., and Kaback, H. R. (1994) *Proc. Natl. Acad. Sci. U.S.A. 91*, 5421−5425.
8. Kaback, H. R. (1996) in *Handbook of Biological Physics: Transport Processes in Eukaryotic and Prokaryotic Organisms* (Konings, W. N., Kaback, H. R., and Lolkema, J. S., Eds.) pp 203−227, Elsevier, Amsterdam.
9. Kaback, H. R., and Wu, J. (1997) *Q. Rev. Biophys. 30*, 333−364.
10. Frillingos, S., Sahin-Tóth, M., Wu, J., and Kaback, H. R. (1998) *FASEB J. 12*, 1281−1299.
11. Kaback, H. R., Voss, J., and Wu, J. (1997) *Curr. Opin. Struct. Biol. 7*, 537−542.
12. Kaback, H. R., and Wu, J. (1999) *Acc. Chem. Res. 32*, 805−813.
13. Frillingos, S., and Kaback, H. R. (1996) *Biochemistry 35*, 3950−3956.
14. Frillingos, S., Wu, J., Venkatesan, P., and Kaback, H. R. (1997) *Biochemistry 36*, 6408−6414.
15. Venkatesan, P., and Kaback, H. R. (1998) *Proc. Natl. Acad. Sci. U.S.A. 95*, 9802−9807.
16. Falke, J. J., Sternberg, D. E., and Koshland, D. E. (1986) *Biophys. J. 49*, 20a.
17. Danielson, M. A., Bass, R. B., and Falke, J. J. (1997) *J. Biol. Chem. 272*, 32878−32888.
18. Butler, S. L., and Falke, J. J. (1998) *Biochemistry 37*, 10746−10756.
19. Bass, R. B., and Falke, J. J. (1998) *J. Biol. Chem. 273*, 25006−25014.
20. Bass, R. B., Coleman, M. D., and Falke, J. J. (1999) *Biochemistry 38*, 9317−9327.
21. Konishi, S., Iwaki, S., Kimura-Someya, T., and Yamaguchi, A. (1999) *FEBS Lett. 461*, 315−318.
22. Kimura, T., Suzuki, M., Sawai, T., and Yamaguchi, A. (1996) *Biochemistry 35*, 15896−15899.
23. Yamaguchi, A., Someya, Y., and Sawai, T. (1992) *J. Biol. Chem. 267*, 19155−19162.
24. Tang, X.-O., Fujinaga, J., Kopito, R., and Casey, J. R. (1998) *J. Biol. Chem. 273*, 22545−22553.
25. Mordoch, S. S., Granot, D., Lebendiker, M., and Schuldiner, S. (1999) *J. Biol. Chem. 274*, 19480−19486.
26. Akabas, M. H., Stauffer, D. A., Xu, M., and Karlin, A. (1992) *Science 258*, 307−310.
27. Stauffer, D. A., and Karlin, A. (1994) *Biochemistry 33*, 6840−6849.
28. Karlin, A., and Akabas, M. H. (1995) *Neuron 15*, 1231−1244.
29. Frillingos, S., and Kaback, H. R. (1997) *Protein Sci. 6*, 438−443.
30. Costello, M. J., Viitanen, P., Carrasco, N., Foster, D. L., and Kaback, H. R. (1984) *J. Biol. Chem. 259*, 15579−15586.
31. Costello, M. J., Escaig, J., Matsushita, K., Viitanen, P. V., Menick, D. R., and Kaback, H. R. (1987) *J. Biol. Chem. 262*, 17072−17082.
32. Li, J., and Tooth, P. (1987) *Biochemistry 26*, 4816−4823.
33. Li, J., and Tooth, P. (1988) *Prog. Clin. Biol. Res. 273*, 93−98.
34. Zhuang, J., Privé, G. G., Verner, G. E., Ringler, P., Kaback, H. R., and Engel, A. (1999) *J. Struct. Biol. 125*, 63−75.
35. Frillingos, S., Sahin-Tóth, M., Persson, B., and Kaback, H. R. (1994) *Biochemistry 33*, 8074−8081.
36. King, S. C., Hansen, C. L., and Wilson, T. H. (1991) *Biochem. Biophys. Acta 1062*, 177−186.
37. Lee, J. L., Hwang, P. P., Hansen, C., and Wilson, T. H. (1992) *J. Biol. Chem. 267*, 20758−20764.
38. Sahin-Tóth, M., Dunten, R. L., Gonzalez, A., and Kaback, H. R. (1992) *Proc. Natl. Acad. Sci. U.S.A. 89*, 10547−10551.
39. Dunten, R. L., Sahin-Tóth, M., and Kaback, H. R. (1993) *Biochemistry 32*, 3139−3145.
40. Sahin-Tóth, M., and Kaback, H. R. (1993) *Biochemistry 32*, 10027−10035.
41. Frillingos, S., and Kaback, H. R. (1996) *Biochemistry 35*, 13363−13367.
42. Voss, J., Sun, J., and Kaback, H. R. (1998) *Biochemistry 37*, 8191−8196.
43. Carrasco, N., Tahara, S. M., Patel, L., Goldkorn, T., and Kaback, H. R. (1982) *Proc. Natl. Acad. Sci. U.S.A. 79*, 6894−6898.
44. Carrasco, N., Viitanen, P., Herzlinger, D., and Kaback, H. R. (1984) *Biochemistry 23*, 3681−3687.
45. Sun, J., Wu, J., Carrasco, N., and Kaback, H. R. (1996) *Biochemistry 35*, 990−998.
46. Sun, J., Frillingos, S., and Kaback, H. R. (1997) *Protein Sci. 6*, 1503−1510.
47. Voss, J., Hubbell, W. L., Hernandez, J., and Kaback, H. R. (1997) *Biochemistry 36*, 15055−15061.
48. Jessen-Marshall, A. E., and Brooker, R. J. (1996) *J. Biol. Chem. 271*, 1400−1404.
49. Wu, J., and Kaback, H. R. (1997) *J. Mol. Biol. 270*, 285−293.
50. Wu, J., Hardy, D., and Kaback, H. R. (1998) *Biochemistry 37*, 15785−15790.
51. Wu, J., Hardy, D., and Kaback, H. R. (1998) *J. Mol. Biol. 282*, 959−967.
52. Carrasco, N., Herzlinger, D., Mitchell, R., DeChiara, S., Danho, W., Gabriel, T. F., and Kaback, H. R. (1984) *Proc. Natl. Acad. Sci. U.S.A. 81*, 4672−4676.
53. Sanger, F., Nicklen, S., and Coulsen, A. R. (1977) *Proc. Natl. Acad. Sci. U.S.A. 74*, 5463−5467.
54. Kaback, H. R. (1971) *Methods Enzymol. 22*, 99−120.
55. Short, S. A., Kaback, H. R., and Kohn, L. D. (1975) *J. Biol. Chem. 250*, 4291−4296.
56. Newman, M. J., Foster, D. L., Wilson, T. H., and Kaback, H. R. (1981) *J. Biol. Chem. 256*, 11804−11808.
57. Careaga, C. L., and Falke, J. J. (1992) *J. Mol. Biol. 226*, 1219−1235.
58. He, M. M., Voss, J., Hubbell, W. L., and Kaback, H. R. (1995) *Biochemistry 34*, 15661−15666.
59. Wu, J., Perrin, D., Sigman, D., and Kaback, H. (1995) *Proc. Natl. Acad. Sci. U.S.A. 92*, 9186−9190.
60. Wu, J., Voss, J., Hubbell, W. L., and Kaback, H. R. (1996) *Proc. Natl. Acad. Sci. U.S.A. 93*, 10123−10127.
61. Wu, J., Hardy, D., Kaback, H. R. (1999) *Biochemistry 38*, 1715−1720.
62. Wu, J., Hardy, D., and Kaback, H. R. (1999) *Biochemistry 38*, 2320−2325.
63. Wang, Q., and Kaback, H. R. (1999) *J. Mol. Biol. 291*, 683−692.
64. Wang, Q., and Kaback, H. R. (1999) *Biochemistry 38*, 16777−16782.
65. Wu, J., Frillingos, S., and Kaback, H. R. (1995) *Biochemistry 34*, 8257−8263.
66. Hubbell, W. L., and Altenbach, C. A. (1994) in *Membrane Protein Structure* (White, S. H., Ed.) pp 224−248, Oxford University Press, New York.
67. Hubbell, W. L., and Altenbach, C. (1994) *Curr. Opin. Struct. Biol. 4*, 566−573.
68. le Coutre, J., Narasimhan, L. R., Patel, C. K., and Kaback, H. R. (1997) *Proc. Natl. Acad. Sci. U.S.A. 94*, 10167−10171.
69. Rastogi, V. K., and Girvin, M. E. (1999) *Nature 402*, 263−268.

BI000438B